


LONG-TERM MONITORING OF METALWORKING FLUID EMULSION AGING USING A SPECTROSCOPIC SENSOR

Cristhiane Assenhaimer ¹, André Salomão Domingos,¹ Benjamin Glasse,² Udo Fritsching² and Roberto Guardani^{1*}

1. Chemical Engineering Department, University of São Paulo, Av Luciano Gualberto Tv3 380, 05508-900 São Paulo SP, Brazil

2. Department of Mechanical Process Engineering, University of Bremen, Badgasteiner Straße 3, 28359 Bremen, Germany

Monitoring of emulsion properties is important in many applications, since aged and broken emulsions perform worse and may affect product quality. Emulsion quality monitoring is a key issue in metalworking fluids (MWF), which are widely used in machining processes, since conventional control methods are not accurate. The present study reports results of the application of a UV-Vis-NIR spectroscopic sensor, coupled with a neural network model, as a new method of monitoring MWF emulsion destabilization, which is related to changes in its droplet size distribution. The technique has shown good accuracy in rebuilding the droplet size distribution of emulsions from spectroscopic measurements, indicating its feasibility to monitor MWF emulsion stability under operating conditions in industrial installations.

Keywords: droplet size distribution, emulsion, metalworking fluid, neural network, UV-Vis-NIR spectroscopy

INTRODUCTION

Emulsions have an important role in a number of industrial sectors, including food, cosmetic, chemical, mining, and mechanical industries, either as products, raw materials, or intermediary in a number of processes. Metal working fluids (MWF) involve a specific class of oil-in-water emulsions with complex formulations that are essential in the manufacturing of pieces by machining processes, since they increase the productivity and reduce costs by enabling the use of higher cutting speeds, higher feed rates, and deeper cuts. The use of MWF can also increase tool life, decrease surface roughness, increase dimensional accuracy and decrease the amount of power consumed in machining operations.^[1] According to the literature, the MWF consumption by a typical machining facility is ~33 t/year.^[2] In 2012, the worldwide consumption was stable at ~2.2 million t/year with a perspective of growth to ca. 2.4 million t/year by 2022,^[3] representing up to 17 % of the total costs of machining processes, while only 2 to 4 % of the total costs are due to the tools.^[4]

The emulsion condition is thus a key issue in the manufacturing processes. In industrial facilities, the status of MWF emulsions is monitored by periodic measurements of some physical-chemical properties, like pH, viscosity, and contamination by micro-organisms. Some facilities adopt a qualitative classification scale based on machine operator perception of the MWF performance, like a colour scale (e.g. green for new fluid, yellow for old fluid, and red for aged fluid). Thus, emulsion status monitoring is dependent on the expertise of machine operators and MWF destabilization may be detected only when it is already affecting the process.

Literature suggests that the monitoring of emulsion destabilization could possibly be used as a better indicator of potential losses in MWF performance.^[5] One possible method deals with the droplet size distribution (DSD), which is directly linked to the quality and physical stability of an emulsion. Figure 1 illustrates typical DSD curves of a fresh metalworking fluid, a metalworking fluid in use, and an aged metalworking fluid. Due to this change in profile, real-time monitoring of the DSD can be used as a

quantitative and sensitive method to detect changes in emulsion properties and to predict changes in MWF performance.

One possible way of monitoring the DSD of an emulsion is by appropriate light scattering techniques like, for example, UV-Vis spectroscopy.^[6–12] Other techniques have also been proposed to monitor DSD in emulsion systems, based on near infrared spectroscopy for emulsion polymerization systems,^[13] on electrical impedance spectroscopy for emulsion stability monitoring,^[14] and more recently on nuclear magnetic resonance and pulsed field gradient measurements applied to DSD monitoring in water-in-oil emulsions.^[15]

The optical models for estimating the DSD in emulsions are based on the treatment of spectroscopic data using the Mie model, from 1908,^[16] which enables to estimate, for known optical properties, the light scattering patterns for a light source interacting with spherical particles of known size dispersed in a medium. Detailed descriptions of the Mie model can be found, for example, in Bohren and Huffman.^[17] Under negligible light absorption conditions, the method relates the measured turbidity of the emulsion, $\tau(\lambda)$ at different wavelengths, λ , with the number-based DSD function, $f(x)$, for droplets with size x , based on Equations (1) and (2).

$$\tau(\lambda) = \frac{1}{L} \ln \left(\frac{I_0}{I} \right) \quad (1)$$

$$\tau(\lambda) = N_p \frac{\pi}{4} \int_0^\infty Q_{\text{ext}}(\lambda, x) x^2 f(x) dx \quad (2)$$

* Author to whom correspondence may be addressed. E-mail address: guardani@usp.br

Can. J. Chem. Eng. 95:2341–2349, 2017

© 2017 Canadian Society for Chemical Engineering

DOI 10.1002/cjce.22931

Published online 20 August 2017 in Wiley Online Library (wileyonlinelibrary.com).

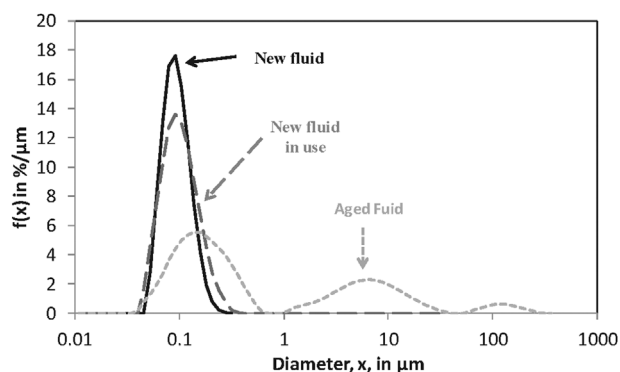


Figure 1. Illustration of changes in droplet size distribution due to emulsion aging.

where L is the optical path length, I_0 is the emitted light intensity, I is the received light intensity, N_p is the total particle number per unit volume, and Q_{ext} is the extinction efficiency, which can be estimated from the Mie theory. Estimation of the DSD, i.e. $f(x)$, from measured data on $\tau(\lambda)$ involves the application of appropriate inversion techniques,^[12,18] which enable the real-time estimation of the DSD, and the in-line monitoring of this emulsion property. However, inversion techniques can generate unstable results, and the optical models for light scattering are not suitable for emulsions with high droplet concentration due to multiple scattering effects.^[7] This is the case of MWF, where the volumetric fraction of oil may reach values between 2 and 10 %.

In a different approach, Reddy and Fogler^[19] showed that, for nearly mono-disperse populations of non-absorbing spheres, the turbidity in Equation (1) is a function of the wavelength only. Deluher and Rajagopalan^[9] used this relationship to propose the use of the so called wavelength exponent, by measuring the turbidity, $\tau(\lambda)$, at different wavelengths, followed by least squares fitting of a straight line of $\ln(\tau(\lambda))$ versus $\ln(1/\lambda)$. The wavelength exponent corresponds to the slope of this fitted straight line. Because of its dependency on the droplet size, by evaluating time changes in the measured spectra the wavelength exponent can be used as an indicator of emulsion stability. In a previous article,^[8] we proposed to generalize the application of this method by showing that, although the wavelength exponent is valid for monodisperse systems only, it can also be used for evaluation of stability of polydisperse systems, with monomodal, and bimodal distributions. Besides, there is no need to exclusively evaluate time-changes in the spectra, since the emulsion stability can also be evaluated by performing instantaneous measurements of turbidity and evaluating the quality of the fitting of the corresponding correlations.

Although the use of the wavelength exponent for evaluating emulsion stability (or destabilization) is easy to be implemented, it performs not so well when applied to droplet populations with high polydispersity, presenting oscillatory behaviour. Therefore, the wavelength exponent was not adopted in this study to evaluate emulsion destabilization, but as an auxiliary criterion, in combination with pattern recognition and classification techniques. This approach can be applied to emulsions under high droplet concentration, and consists of associating the spectral data measured by the spectroscopic sensor with the corresponding DSD by means of a previously calibrated multivariate model. Among different techniques that can be applied, non-linear models such as neural networks have been successfully applied by the present authors in place of light scattering models to estimate size

distributions in concentrated solid-liquid suspensions^[20,21] and to evaluate changes in DSD by light scattering during artificial aging of MWF emulsions.^[7]

The specific contribution of this study consists in proposing the use of a neural network-based technique to estimate the DSD of MWF emulsion samples monitored by an in-line UV-Vis-NIR spectroscopic sensor over a relatively long operation period of a machining facility, and the use of this information to evaluate the MWF condition. This approach is based on previous studies by the authors with laboratory prepared emulsions,^[7,8] and is here applied to the long-term monitoring of MWF under operating conditions of large scale machining facilities.

MATERIALS AND METHODS

Experimental

In order to obtain data as near as possible to a real case scenario, a set of emulsion samples from 7 commercial metalworking fluids (Acmosit 65-66, from Acmos Chemie KG; Grindex 10, from Blaser Swisslube; Unimet 230 BF, from Oemeta; Rhenus r. meta TS 42, rhenus XY 121 HM and rhenus R-Flex, from Rhenus Lub; Zubora 10 M Extra, from Zeller-Gmelin) were monitored for a period of 13 months while being used in 3 different machines in a machining facility (a vertical turning machine, Index C200-4D, a precision milling machine, Sauer 20 linear, and a cylindrical grinding machine, Overbeck 600 R-CNC). All these MWF are oil-in-water emulsions, made from synthetic oils and several additives to fulfill the purpose of emulsification, corrosion inhibition, and microbial control, among others. Each emulsion was previously diluted to the recommended concentration for the corresponding application, i.e. with concentration of the oil phase between 2 and 10 %. Since water can evaporate during the operation period, adjustments in concentration were carried out by the operating personnel when the total MWF volume decreased by about 5 %.

The sampling procedure involved the collection of ca. 100 mL of the emulsion from the circulation tank of each machine in a glass flask. One sample per week was collected from each machine over the 13 month period, resulting in a total of 156 samples. Periodic analyses of physico-chemical and microbiological properties of the fluid (pH, concentration, nitrite concentration, and microbiological contamination by ATP method, according to German regulation requirements) were performed over the operation time as a routine of the operation personnel, with supervision by this research team. Light extinction spectra measurements were carried out for all samples by means of a UV-Vis-NIR spectrometer, model HR2000 + ES, from OceanOptics, with a DH 2000-BAL (200–1100 nm) light source, and a deep probe with 6.35 mm diameter, 127 mm of length, and 2 mm optical path, which enables in-line monitoring. The light extinction spectra were used for the calculation of the wavelength exponent of the samples, as previously described. The linear coefficient of the fitted straight line was also included in the collected dataset. Although this coefficient itself does not have a physical meaning, it is related to the concentration and optical properties of the analyzed samples, and can be used to distinguish different fluids. The raw spectral data, i.e. the measured absorbance at each wavelength within the analyzed wavelength range, were also used in the last part of this study without further treatment. The droplet size distributions (DSD) of the samples were measured in a Malvern Mastersizer 2000 laser diffractometer, with particle size detection range from

0.02 to 2000 μm . This information was adopted as a reference in the fitting of neural network models.

The measured variables used in the study are as follows:

- Variables monitored in the machining facility:
 - pH;
 - Concentration of the fluid, measured in wt%;
 - Nitrite content in the MWF, measured in mg/L;
 - Microbiological contamination by ATP method, expressed as $\log(\text{ATP})$ and measured in CFU/mL (colony forming units per mL).
- Variables monitored via the spectroscopic sensor:
 - Wavelength exponent of the samples, z , calculated between 500–600 nm;
 - Linear coefficient of the wavelength exponent fitting, which is related to the optical properties of the fluid and emulsion concentration.
- Reference measurements:
 - Volumetric mean diameter $D_{4,3}$, calculated from the obtained DSD, as measured in a Malvern Mastersizer diffractometer.

Classification of the MWF Status

The machine operating personnel classified the collected MWF samples according to a conventional classification criterion, which is based on the machine operator perception of fluid quality as: Status 1 (no signs of deterioration), Status 2 (initial signs of deterioration), and Status 3 (high degree of deterioration). This qualitative classification by operators is one of the determinant factors in deciding when a MWF emulsion can be considered aged and has to be disposed and replaced. The results obtained with this classification criterion were compared with those obtained with a quantitative multivariate classification criterion, consisting of linear and quadratic discriminants.^[22]

Discriminant analysis is based on G groups of multivariate observations with dimension p , i.e. consisting of p variables. The probability density function, $\Phi_g(\mathbf{x})$, corresponding to the normal distribution of observations in a given group g is expressed by Equation (3), where $g = 1, 2, \dots, G$. In the present case, each group corresponds to one Status, thus G is equal to 3.

$$\Phi_g(\mathbf{x}) = \frac{1}{(2\pi)^{p/2} |\mathbf{V}_g|^{1/2}} \exp \left[-\frac{1}{2} (\mathbf{x} - \boldsymbol{\mu}_g)^T \mathbf{V}_g^{-1} (\mathbf{x} - \boldsymbol{\mu}_g) \right] \quad (3)$$

By assuming that each group has its own covariance matrix, \mathbf{V}_g , and that the observations in each group are normally distributed, the criterion for allocation of observations is based on the product of the a priori probability of occurrence of a given group, π_g , and the probability density function, $\pi_g \cdot \Phi_g(\mathbf{x})$, for each group. For this purpose, the linearized form of the normal probability density function is more conveniently used, and Equation (3) can be rewritten as Equation (4).

$$\ln[\pi_g \Phi_g(\mathbf{x})] = \ln(\pi_g) - \left(\frac{p}{2}\right) \ln(2\pi) - \frac{1}{2} \ln|\mathbf{V}_g| - \frac{1}{2} (\mathbf{x} - \boldsymbol{\mu}_g)^T \mathbf{V}_g^{-1} (\mathbf{x} - \boldsymbol{\mu}_g) \quad (4)$$

Since the second term of the right-hand side of the equation is the same for all groups, the comparison between groups is based on the remaining terms, and the so-called quadratic discriminant is expressed as Equation (5).

$$\text{discr} \cdot Q_g(\mathbf{x}) = \ln(\pi_g) - \frac{1}{2} \ln|\mathbf{V}_g| - \frac{1}{2} (\mathbf{x} - \boldsymbol{\mu}_g)^T \mathbf{V}_g^{-1} (\mathbf{x} - \boldsymbol{\mu}_g) \quad (5)$$

According to this criterion, a given observation \mathbf{x}_0 is allocated in the group for which the value of $\text{discr} \cdot Q_g(\mathbf{x}_0)$ is maximum. The discriminant is denominated quadratic due to the quadratic statistical distance in the equation. In the linear discriminant analysis (LDA) the covariance matrices are assumed to be equal for all groups. Therefore, Equation (5) can be rewritten for expressing the linear discriminant as shown in Equation (6), which includes the terms that depend on each group, only.

$$\text{discr} \cdot \text{Lin}_g(\mathbf{x}) = \ln(\pi_g) + \boldsymbol{\mu}_g^T \mathbf{V}^{-1} \mathbf{x} - \frac{1}{2} \boldsymbol{\mu}_g^T \mathbf{V}^{-1} \boldsymbol{\mu}_g \quad (6)$$

In this study, LDA and QDA were used to classify the samples in Status 1, 2, or 3 based on the measured variables, using the statistical software Minitab. All evaluations were based on cross-validation, which is based on the exclusion of one or more observations from the data set used to estimate the discriminant, and testing the criterion with the excluded observations.

Neural Network Fitting

A description of the neural network model and the fitting method adopted in this study was presented in a previous article by the authors.^[7] A three-layer feed-forward neural network was used to estimate the DSD of the samples based on the measured variables.

In this study, the output of each neuron j in the network, O_j , is a sigmoidal function of the weighted sum, S_j , as shown in Equation (7).

$$O_j = \frac{1}{1 + e^{-S_j}}, \quad (7)$$

in which S_j represents the weighed sum of the inputs to neuron j , i.e. the following:

$$S_j = \sum_{i=1}^q W_{ij} X_i + W_{q+1,j} \quad (8)$$

The dataset was divided into a training set, with ca. 2/3 of the data, and a validation set, with the remaining 1/3 of the data. The training consisted of fitting the weights to each neuron, $W_{i,j}$, and was carried out according to the backpropagation algorithm.^[23] The usual minimization criterion, i.e. the squared error E , is defined in Equation (9), where y_k is the experimental value of output k and O_k is the calculated value of output k at interaction m .

$$E = \sum_{\text{all observations}} \sum_{k=1}^p \left(y_k^{(m)} - O_k^{(m)} \right)^2 \quad (9)$$

In this study, this criterion was modified in order to increase the importance of the droplet population formed by the larger coalesced droplets by expressing the error in the form of Equation (10), where A_{calc} is the area under the calculated DSD curve, and A_{exp} is the area under the experimental DSD curve.

$$E = \sum_{\text{observations}} \sum_{k=1}^{p-1} \left(A_{\text{calc},k}^{(m)} - A_{\text{exp},k}^{(m)} \right)^2 \quad (10)$$

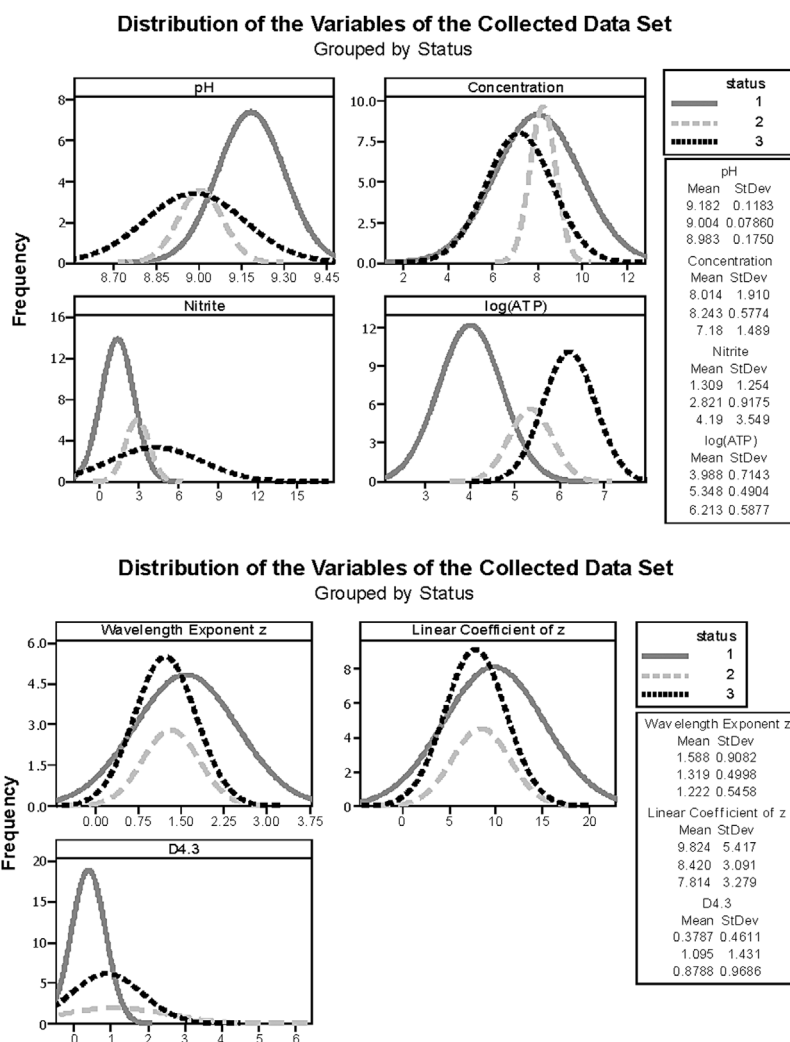


Figure 2. Distribution of variables of the collected samples, for each status. (Concentration in %, nitrite in mg/L, microbiological contamination in CFU/mL, and D_{4.3} in μm).

where

$$A_{calc,k} = \left(\frac{O_{k+1} - O_k}{2} \right)^2 \cdot \Delta x_k \quad (11)$$

$$A_{exp,k} = \left(\frac{y_{k+1} - y_k}{2} \right)_{exp}^2 \cdot \Delta x_k \quad (12)$$

The reason is that the size intervals, Δx_k , used in the DSD increase with size as multiples of $\sqrt{2}$, and are thus larger for larger droplet sizes. This makes the squared error, Equation (10), more sensitive to the presence of the larger coalesced droplets. The computational programs for neural network model fitting, validation, and simulations were developed in the Chemical Engineering Department, University of São Paulo.

Table 1. Predictors and results of the application of discriminants to the data

	Fitting 1	Fitting 2	Fitting 3	Fitting 4	Fitting 5	Fitting 6
Predictors	pH Concentration Nitrite Log(ATP) –	pH Concentration Nitrite Log(ATP) Wavelength Exponent –	pH Concentration Nitrite Log(ATP) Wavelength Exponent Linear Coefficient of Wavelength Exponent Fitting	pH Concentration – – Wavelength Exponent –	pH Concentration – – Wavelength Exponent Linear Coefficient of Wavelength Exponent Fitting	– – Nitrite Log(ATP) – –
Efficiency, Linear Discriminant	80 %	80 %	81 %	55 %	53 %	80 %
Efficiency, Quadratic Discriminant	80 %	78 %	81 %	58 %	62 %	81 %

RESULTS AND DISCUSSION

Status Classification by the Operators

The distribution of measured variables according to each status based on the classification made by the machine operators is

shown in Figure 2. There is no clear association between the measured variables and the status of the fluid. The only clearly observed tendency is that samples classified as Status 1, corresponding to emulsions without signs of deterioration, show higher pH values than samples with Status 2 or 3. However,

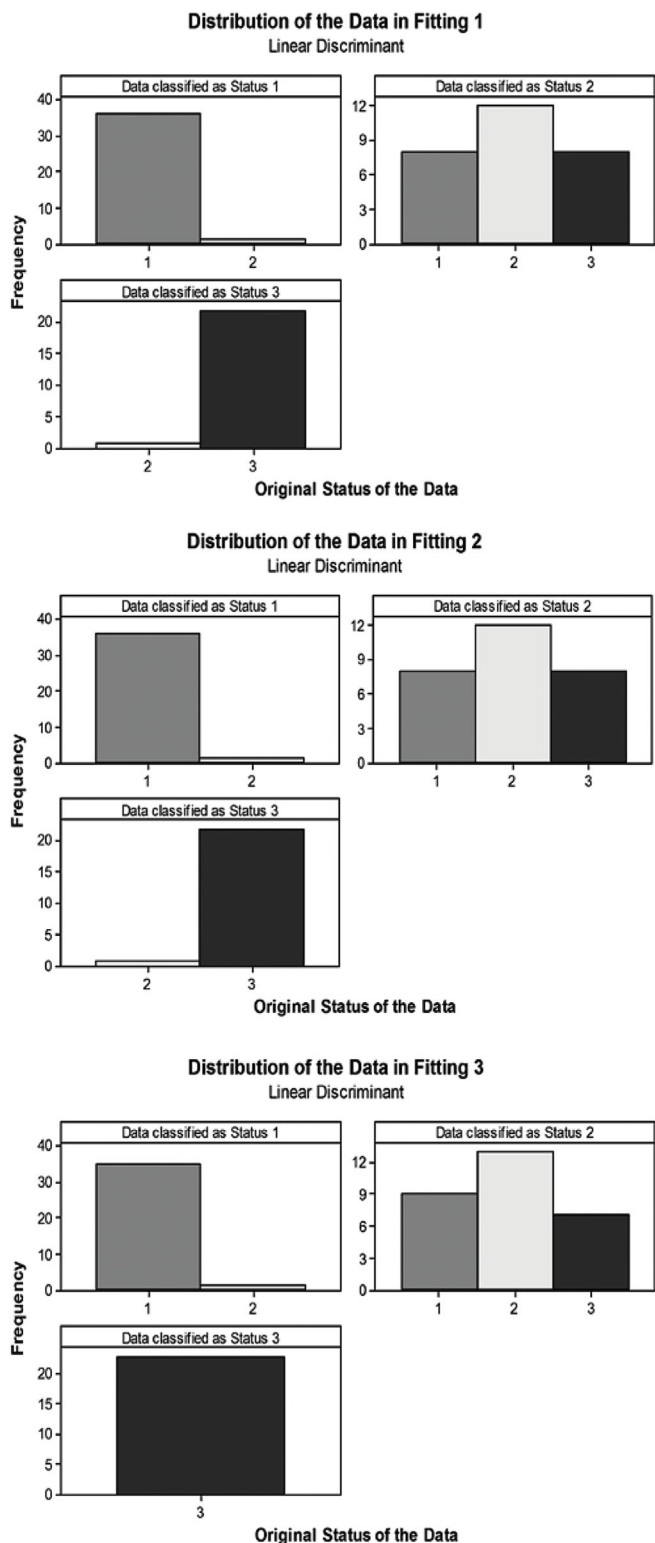


Figure 3. Frequency distribution of the data classified by Linear Discriminant for each original status (horizontal axis, as classified by the operating personnel).

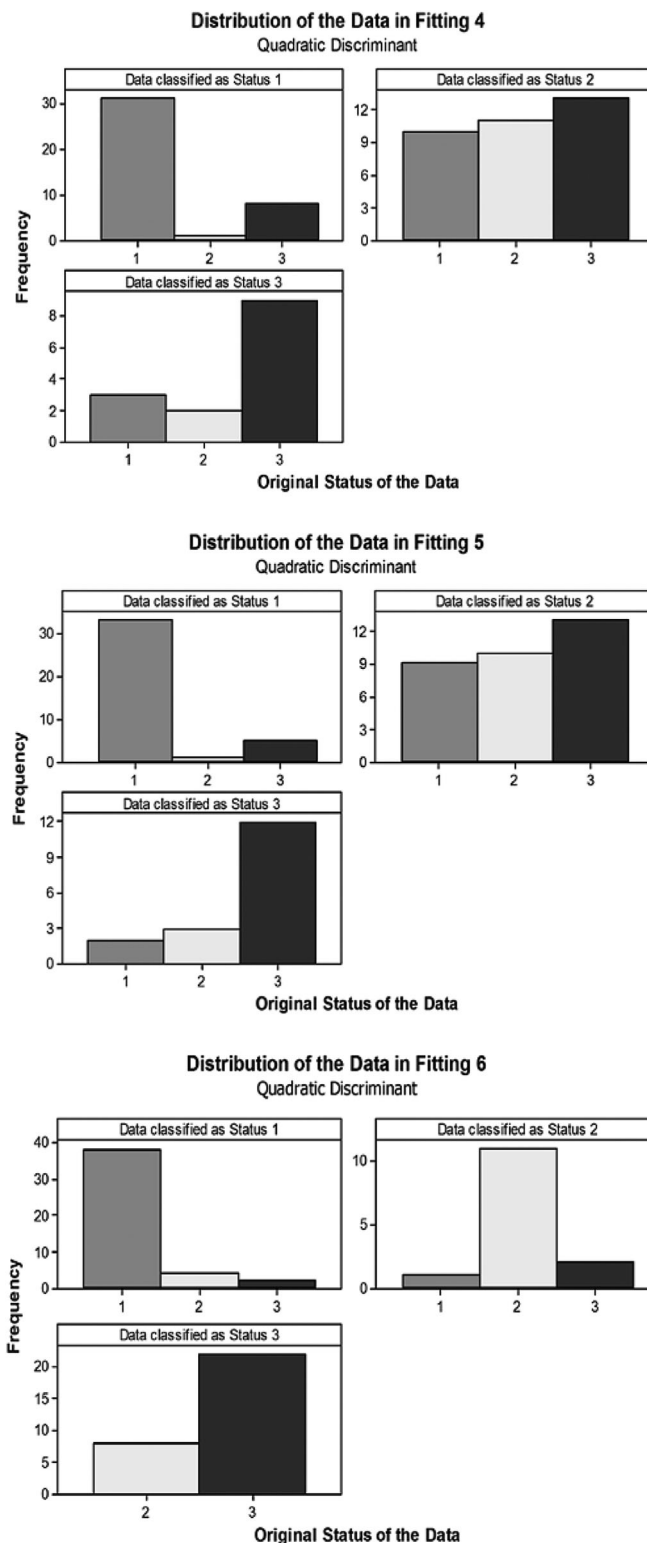


Figure 4. Frequency distribution of the data classified by Quadratic Discriminant for each original status (horizontal axis, as classified by the operating personnel).

a large variance is observed. The microbiological contamination, expressed as $\log(\text{ATP})$, shows some correlation with status, since the increase in microbiological contamination is associated with the degradation of the fluid. Anaerobic bacteria degrade nitrate or nitrite to ammonia and sulphate or sulphonate to hydrogen sulphide, causing unpleasant odours, so the monitoring of nitrite content in the MWFs is also required by specific legislation applied to machining industry.^[24] Emulsions with higher nitrite content can show altered levels of odour, so it was indeed expected to find higher values of this variable in samples classified as Status 3, i.e. with higher signs of deterioration. The corresponding plot in Figure 2 shows a larger variance for the nitrite content in Status 3 samples.

Concerning the distribution of the volumetric mean diameter ($D_{4,3}$), Figure 2 shows that samples with Status 1 have smaller $D_{4,3}$

values, as expected. However, for samples with Status 2 and Status 3 the difference is not clear, since both have larger $D_{4,3}$ values and larger variances.

Status Classification by Discriminant Analysis

The variables adopted in the monitoring of the MWF by the operation personnel (pH, concentration, nitrite content, and microbiological contamination by ATP method) were included in the classification based on discriminant analysis. The efficiency of the classification method was based on the fraction of correctly classified observations in the original status. Here, the denomination original status refers to each of the three status resulting from the classification made by the machine operating personnel, as described previously. Besides the mentioned variables, the wavelength exponent and the linear coefficient of the linearly

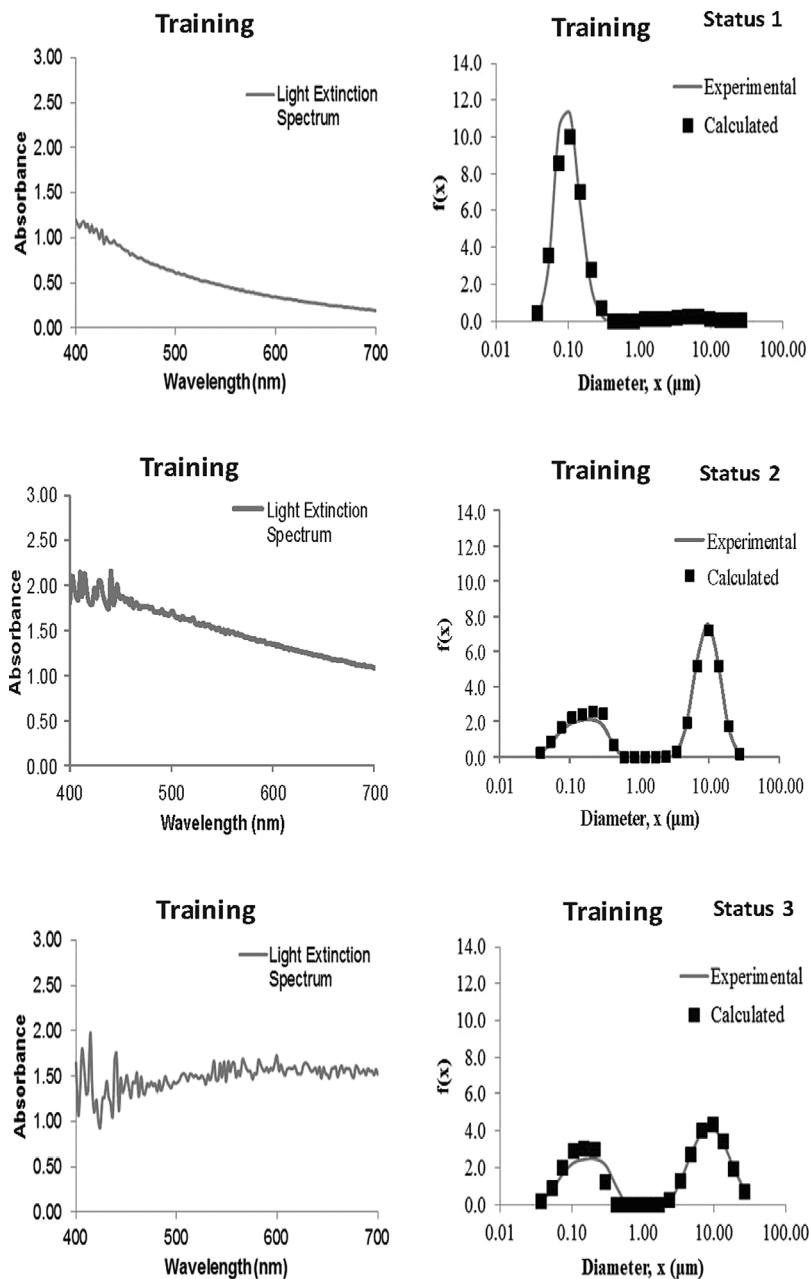


Figure 5. Neural network fitting results for the long-term monitoring study of commercial MWFs in a machining facility, using the fitting criterion described in Equations (10) to (12), with 12 inputs and 20 outputs. Plots on the left: light extinction spectrum; plots on the right: experimental and calculated droplet size distribution (volumetric %).

adjusted spectral data were also included as predictors. Linear and quadratic discriminants were tested for six different sets of variables, as listed in Table 1, which also shows the resulting efficiency for each fitting.

The highest efficiency obtained was 81 % for both linear and quadratic discriminants. The inclusion of nitrite content and microbiological contamination, as log (ATP), in the group of predictors resulted in an increase in the classification efficiency, indicating that the microbiological contamination is an important factor affecting the classification of the MWF emulsion status. However, since the maximum efficiency was 81 %, even when other variables were used as additional predictors, it seems that other non-monitored factors may affect MWF emulsion classification.

Figures 3 and 4 show the distribution of the original status of the samples for each status classified by discriminant analysis, and for all fittings. These results indicate that there is a reasonable agreement between discriminant analysis and the criterion adopted by the operators to classify the MWF samples in Status 1 or Status 3. However, there is much disagreement in the classification in Status 2, which corresponds to MWF samples with initial signs of deterioration. This disagreement can be caused by misclassification by the operators, or by any other unmeasured factor that may affect the MWF behaviour.

These results indicate the need for a more efficient approach to identify the MWF emulsion condition. Based on the fact that emulsion destabilization is associated with droplet coalescence, and on previous results obtained by the authors with a

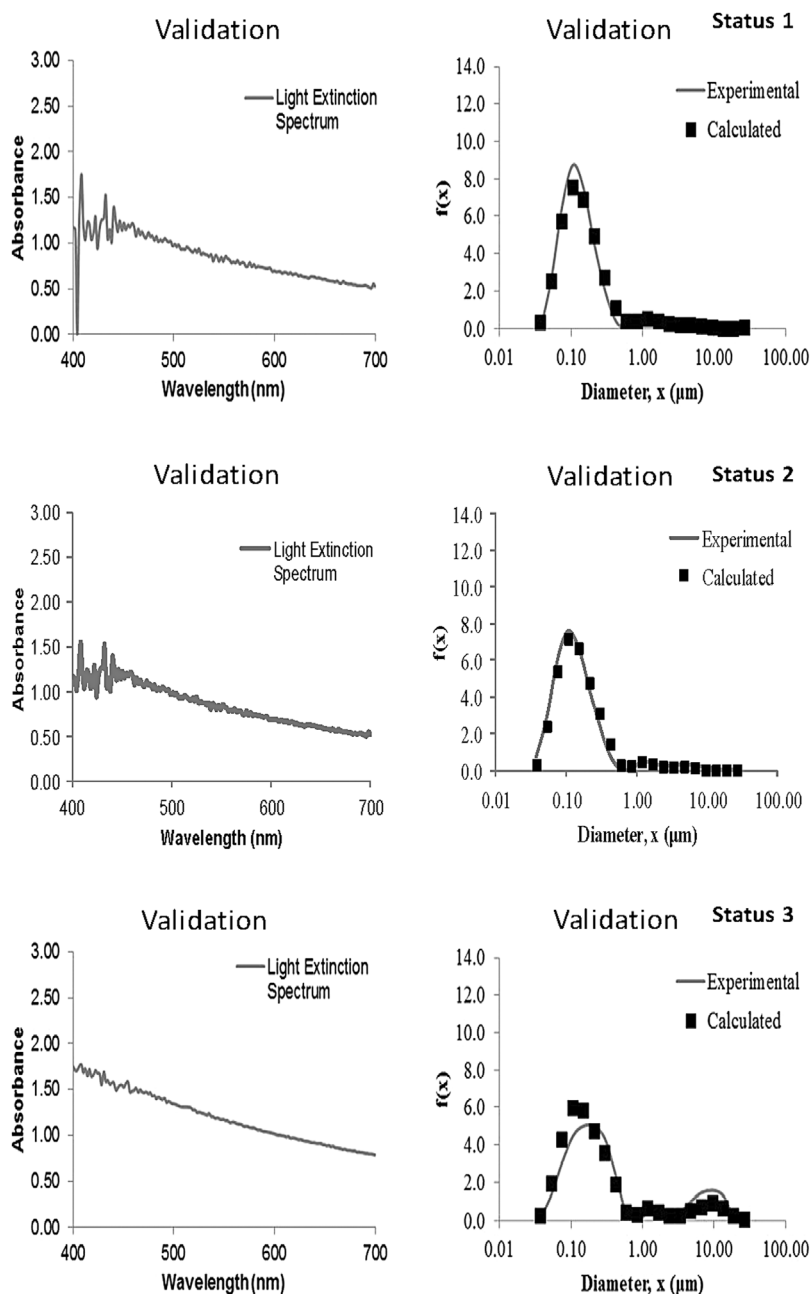


Figure 6. Neural network validation results for the long-term monitoring study of commercial MWFs in a machining facility, using the fitting criterion described in Equations (10) to (12), with 12 inputs and 20 outputs. Plots on the left: light extinction spectrum; plots on the right: experimental and calculated droplet size distribution (volumetric %).

spectroscopic sensor coupled with a neural network to estimate the droplet size distribution in MWF emulsions,^[7,8] a similar approach was applied to the operation data for evaluating MWF status, as explained in the next item.

Coupling of the Spectroscopic Sensor and a Neural Network Model for the Monitoring of MWF Emulsion Destabilization

The three-layer feed-forward neural network that was fitted to the experimental data comprised 12 input variables: 8 absorbance values arbitrarily selected in 40 nm intervals, in the range of 402 nm to 690 nm, MWF concentration, pH, calculated value for the wavelength exponent, and the linear coefficient obtained in the least squares fitting of the wavelength exponent to the spectral data. Although the linear coefficient does not appear to have a physical meaning, it is related to the optical properties of the fluids and apparently can help to discriminate the spectra from different fluids. In fact, the optical properties of these fluids would be a more suitable option, but it was not possible to have access to this information, especially because they are formulated from a wide range of different substances, and the formulation itself is not made available by the MWF producers. As outputs of the neural network, 20 size classes were selected, from 0.04 μm to 26.7 μm , as multiples of $\sqrt{2}$, arbitrarily adopted in order to reconstruct the DSD of the samples with appropriate resolution. For the neural network fitting, $\sim 30\%$ of the data were used in model validation. A total of 50 000 presentations of the dataset to the neural network were adopted in each fitting, and the best fitting was obtained with 10 neurons in the hidden layer

Figures 5 and 6 show the results of the neural network fitting for samples with different aging times, and consequently different Status classifications, representative of the whole set. The plots on the left show the light extinction spectrum of each MWF emulsion, as measured with the spectroscopic sensor, and the plots on the right show the corresponding DSD for the measured distribution, and for the distribution calculated by the model. Although the measured spectra change with the destabilization of the emulsion, the tendency of such changes cannot be observed from the spectra directly. However, the fitting of the neural network to the data resulted in good agreement between calculated and experimental values of the DSD curves for all samples with monomodal and bimodal distributions, by using the same fitted neural network model for all cases. From these results, it is clear that the classification of the MWF emulsion samples in Status 1 corresponds to monomodal DSD curves, composed of a population of small droplets. However, the classification criterion is not efficient for Status 2 or 3, since the samples show the presence of the second mode in the DSD plots, possibly caused by droplet coalescence. As previously described, this neural network model is based on data generated in real time by the spectroscopic sensor placed in-line, plus other inputs that can be easily obtained in machining processes. Thus, a system consisting of the spectroscopic sensor coupled with a neural network model can be used to detect the emulsion destabilization in its early steps, based on the presence of the second droplet population. Such a system can be applied to in-line and real-time measurements.

CONCLUSIONS

In this study, an alternative approach is proposed for real-time monitoring of emulsion destabilization, based on the use of a spectroscopic sensor and a neural network model. The information provided in real time by the sensor, i.e. the light extinction spectrum, is used as input to a neural network model, which

estimates the droplet size distribution of the dispersed phase, which is directly linked to the quality and physical stability of an emulsion. This information enables the monitoring of changes in the emulsion structure that can be associated with the destabilization process. The method was tested in a long-term monitoring study of commercial metal working fluid emulsions in a machining facility, by comparing the results with a status classification criterion adopted by operation personnel, based on routine analyses and experience. Good agreement between calculated and experimental values of the droplet size distribution was achieved for samples with monomodal and bimodal distributions.

The results indicate that a system consisting of the spectroscopic sensor coupled with a neural network model can be used to detect the emulsion destabilization in its early steps, by associating this with the presence of a second droplet population with larger droplets. Such a system can be adjusted for in-line and real-time measurements, since the spectroscopic sensor can be placed in different locations inside the equipment, e.g. in tubes or in vessels. This is a new method for monitoring emulsions with possible applications in similar systems in food industries, emulsion polymerization processes, crystallization processes, among others.

ACKNOWLEDGEMENTS

This study is part of a joint project between the Universities of São Paulo and Bremen, within the BRAGECRIM program (Brazilian German Cooperative Research Initiative in Manufacturing). The authors would like to thank FAPESP, CAPES, FINEP, and CNPq (Brazil), and DFG (Germany) for the financial support.

NOMENCLATURE

A	area under the droplet size distribution curve at a given size interval (m^2)
$D_{4.3}$	volumetric mean droplet size (nm)
$discr.Lin$	linear discriminant, defined in Equation (6)
$discr.Q$	quadratic discriminant, defined in Equation (5)
E	squared error, defined in Equations (9) to (12)
$f(x)$	number-based droplet size distribution (DSD) density function (nm^{-1})
G	number of groups in discriminant analysis
I	measured light intensity (W m^{-2})
I_0	intensity of the light source (W m^{-2})
L	optical path (m)
N_p	total number of droplets per unit volume (m^{-3})
O_j	output of neuron j
O_k	calculated value of output k
Q_{ext}	extinction efficiency
p	number of variables of each observation in discriminant analysis
q	number of inputs to the neural network
S_j	weighted sum of inputs to a neuron in a neural network, defined in Equation (7)
V	covariance matrix of observations
$W_{i,j}$	weights applied to the connection between neurons i and j in a neural network
x	droplet size (nm)
\mathbf{x}	column vector of a given observation of the p variables
X	input variables to a model
x_j	original variables

X_{q+1}	bias
y_k	experimental value of output k of a neural network
z	wavelength exponent
τ	turbidity

Subscriptps

g	group index in the discriminant analysis
i	refers to input i to a neural network
j	index for a neuron in a feedforward neural network
k	refers to output k of a neural network

Greek Letters

λ	wavelength (nm)
Φ	probability density function
μ	column vector of the mean value of observations (with dimension p)
π	a priori probability of occurrence

REFERENCES

- [1] M. A. El Baradie, *J. Mater. Process. Tech.* **1996**, 56, 786.
- [2] J. F. G. De Oliveira, S. M. Alves, *Produção* **2007**, 17, 129.
- [3] M. Phadke, *Tribol. Lubr. Technol.* **2014**, 3, 38.
- [4] C. Cheng, D. Philips, R. M. Alkhaddar, *Water Res.* **2005**, 39, 4051.
- [5] F. Klocke, G. Eisenblätter, *CIRP Ann.-Manuf. Tech.* **1997**, 46, 519.
- [6] M. Greeley, N. Rajagopalan, *Tribol. Int.* **2004**, 37, 327.
- [7] C. Assenhaimer, L. J. Machado, B. Glasse, U. Fritsching, R. Guardani, *Can. J. Chem. Eng.* **2014**, 92, 318.
- [8] B. Glasse, C. Assenhaimer, R. Guardani, U. Fritsching, *Chem. Eng. Technol.* **2013**, 36, 1202.
- [9] J. Deluhery, N. Rajagopalan, *Colloid. Surface. A* **2005**, 256, 145.
- [10] G. E. Elicabe, L. H. Garcia-Rubio, *Adv. Chem. Ser.* **1990**, 227, 83.
- [11] M.-T. Celis, L. H. Garcia-Rubio, *J. Disper. Sci. Technol.* **2002**, 23, 293.
- [12] M.-T. Celis, L. H. Garcia-Rubio, *J. Disper. Sci. Technol.* **2008**, 29, 20.
- [13] W. K. Silva, D. L. Chicoma, R. Giudici, *Polym. Eng. Sci.* **2011**, 51, 2024.
- [14] S. Shahidi, C. R. Koch, S. Bhattacharjee, M. Sadrzadeh, *Sensor. Actuat. B-Chem.* **2017**, 243, 460.
- [15] N. N. A. Ling, A. Haber, E. F. May, E. O. Fridjonsson, M. L. Johns, *Chem. Eng. Sci.* **2017**, 160, 362.
- [16] G. Mie, *Ann. Phys.* **1908**, 25, 377.
- [17] D. Bohren, C. F. Huffman, *Absorption and Scattering of Light by Small Particles*, John Wiley & Sons, New York **1983**.
- [18] M.-T. Celis, L. H. Garcia-Rubio, *Ind. Eng. Chem. Res.* **2004**, 43, 2067.
- [19] S. R. Reddy, H. S. Fogler, *J. Colloid Interf. Sci.* **1981**, 79, 101.
- [20] R. Guardani, C. A. O. Nascimento, R. S. Onimaru, *Powder Technol.* **2002**, 126, 42.
- [21] C. A. O. Nascimento, R. Guardani, R. M. Giuletti, *Powder Technol.* **1997**, 90, 89.

- [22] R. A. Johnson, D. W. Wichern, *Applied Multivariate Statistical Analysis*, 6th edition, Prentice-Hall, Upper Saddle River **2007**.
- [23] D. Rummelhart, J. McClelland, *Parallel Distributed Processing Explorations in the Microstructure of Cognition, 1*, MIT Press, Cambridge **1986**, p. 567.
- [24] J. P. Byers, *Metalworking Fluids*, 2nd edition, CRC Press, Boca Raton **2006**.

Manuscript received January 4, 2017; revised manuscript received May 3, 2017; accepted for publication May 6, 2017.